THE ASTROPHYSICAL JOURNAL, 277:43–50, 1984 February 1

1E 0104.2+3153: A BROAD ABSORPTION-LINE QSO VIEWED THROUGH A GIANT ELLIPTICAL GALAXY[1]

J. T. STOCKE AND JAMES LIEBERT
Steward Observatory, University of Arizona

AND

R. SCHILD, I. M. GIOIA,[2] AND T. MACCACARO[2]
Harvard-Smithsonian Center for Astrophysics
Received 1983 June 9; accepted 1983 July 25

ABSTRACT

The optical identification of the X-ray source 1E 0104.2+3153 is complicated by the close projection of a broad absorption-line (BAL) QSO ($z = 2.027$) 10″ from a giant elliptical galaxy ($z = 0.111$) at the center of a compact group of galaxies. At only 1.2 de Vaucouleur radii (16 kpc for $H_0 = 100$ km s^{-1} Mpc^{-1}) this QSO-galaxy projection is the closest yet discovered. Based upon current observations, the source of the X-ray emission cannot be conclusively determined. Present in the BAL QSO spectrum are extremely strong Ca II H and K absorption lines due to the intervening galaxy, the first optical detection of the cold interstellar medium in an elliptical galaxy. The strength of these lines (EW = 2 and 1 Å) requires that we are looking through several interstellar clouds in the line of sight to the QSO. By its proximity to the central regions of the elliptical galaxy and the relative distances of the galaxy and QSO, this QSO is a particularly good candidate for observing dramatic transient gravitational lensing phenomena due to halo stars in the foreground galaxy.

Subject headings: galaxies: individual — interstellar: matter — quasars — X-rays: sources

I. INTRODUCTION

As part of a systematic search for serendipitous X-ray sources to extend the *Einstein Observatory* Medium Sensitivity Survey, we have analyzed an X-ray image centered on 3C 31 (=NGC 383). In the imaging proportional counter (IPC) field a serendipitous source, 1E 0104.2+3153, was detected at $01^h04^m13^s.9$, $+31°53'31''.7$ (epoch 1950.0). A full description of the Medium Sensitivity Survey and of the optical identification of its sources is given elsewhere (Maccacaro *et al.* 1982; Stocke *et al.* 1983*b*; Gioia *et al.* 1984). In this paper we present a detailed discussion of 1E 0104.2+3153 since the X-ray error circle contains the close projection (10″) of a broad absorption-line QSO at $z = 2.027$ and a bright elliptical galaxy at $z = 0.111$ (Fig. 1 [Plate 1]). The true identity of the X-ray source is still ambiguous because of the size of the IPC error circle, which is larger (30″) than the projected separation between the QSO and the galaxy.

Systems containing a QSO in near alignment with a galaxy are interesting for three reasons:

1. There appears to be a statistical excess of QSOs near bright galaxies (Burbidge *et al.* 1971; Arp 1981), which has been interpreted as evidence of physical association. However, recent work suggests an alternative explanation for this excess; viz., gravitational lensing by halo stars belonging to the foreground galaxy brighten the QSO image making the association appear more unlikely than it really is (see 3 below; Canizares 1981; Keel 1982). The QSO galaxy pair reported here is the closest projection yet found.

2. The light of the QSO becomes a probe of the diffuse matter in the outer portions of the galaxy. Existence of interstellar absorption lines produced by a nearby intervening galaxy has been discovered in three QSO spectra (3C 232, Boksenberg and Sargent 1978 and Haschick and Burke 1975, in H I; PKS 2020−370, Boksenberg *et al.* 1980; and 0446−208, Blades, Hunstead, and Murdock 1981). We report here the fourth such case and the first due to an elliptical galaxy.

3. The close coincidence of the QSO light path with stars in the galaxy halo offers the possibility of observing dramatic transient gravitational lensing phenomena (Chang and Refsdal 1979; Gott 1981; Young 1981; Canizares 1981; Keel 1982). The relative distances of the QSO and galaxy in this particular case suggest flares on a time scale of a few years with a greater than 1% probability that a flare is in progress. Clearly this particular alignment warrants continued optical monitoring.

Section II discusses the X-ray source and its identification, § III the photometric observations of the field, § IV the optical spectra including the detection in the QSO spectrum of Ca II H and K absorption due to the galaxy, and § V the possible gravitational lensing of the QSO by individual halo stars. Throughout this paper, $H_0 = 100$ km s^{-1} Mpc^{-1} is assumed.

II. THE X-RAY SOURCE IDENTIFICATION

1E 0104.2+3153 was detected at the 6 σ confidence level with a flux of 4.0 (±0.7) × 10^{-13} ergs cm^{-2} s^{-1} in the 0.3–3.5 keV X-ray band in an IPC field taken on 1980 June 30. The centroid of the 30″ (90% confidence) error circle is marked with a plus sign in Figure 1. Present in the error circle are a large elliptical galaxy (the dominant member of a small group of galaxies), three compact galaxies which are members of this

[1] Research reported here used the Multiple Mirror Telescope Observatory, a joint facility of the Smithsonian Institution and the University of Arizona.
[2] Also from the Istituto di Radioastronomia, CNR, Bologna, Italy.

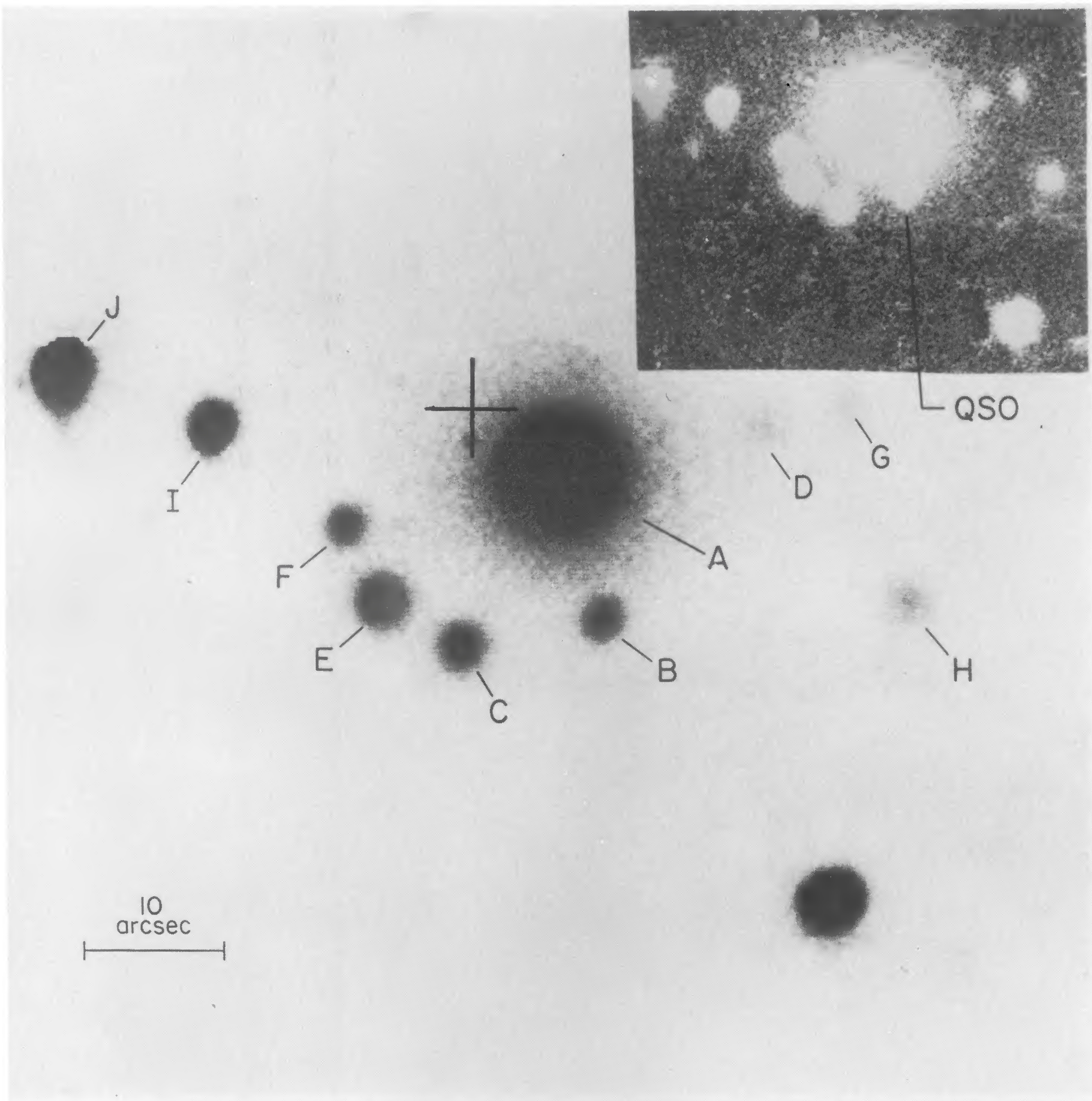

FIG. 1.—The field of the X-ray source 1E 0104.2+3153. This 10 minute exposure was taken on the MMT on the night of 1982 February 21 through an F filter with $\lambda c = 6500$ Å and $\Delta\lambda = 1500$ Å onto an RCA CCD (see Schild and Kent 1981 for details). North is up, and east is to the left. The insert shows the same CCD frame at higher contrast, emphasizing that the QSO is embedded within the halo of galaxy A. The + sign marks the X-ray centroid, which has a 30″ 90% confidence error circle. The labeled objects are individually identified in Table 1.

STOCKE *et al.* (*see* page 43)

TABLE 1

PROPERTIES OF SOURCES IN 1E 0104.2+3153 FIELD

Source	Identification	R.A. (1950.0)	Decl. (1950.0)	R mag	z
A	elliptical galaxy	$1^h04^m13^s.42$	+31°53′26″.7	15.13	0.1115
B	QSO	13.20	16.7	18.88	2.027
C	galaxy	13.88	15.2	18.34	0.11
D	galaxy	11.88	15.9	20.90	...
E	galaxy	14.33	18.0	17.91	0.11
F	galaxy	14.52	22.9	18.71	0.11
G	galaxy	11.58	19.0	20.23	...
H	galaxy	...	...	19.48	...
I	K star	15.18	29.5	17.48	...
J	G star	16.13	33.2	[a]	...
X-ray source	...	13.9	31.7	...	...

[a] Magnitude not well determined because object J is at the edge of the CCD field.

small group, and the QSO. Also inside the error circle are two stars which, on the basis of their X-ray to visual flux ratio f_x/f_v (see Maccacaro *et al.* 1982 and Stocke *et al.* 1983*b*), are ruled out as the optical counterpart of the X-ray source. Identifications for the labeled objects in Figure 1 as well as positions (±0″.5), R magnitudes (±0.1 mag), and redshifts are given in Table 1.

Since both QSOs and groups of galaxies with richness and morphology similar to this group have been identified as the optical counterparts to X-ray sources in this flux range (e.g., Stocke *et al.* 1983*b*), neither the QSO nor the group can be confidently eliminated as the X-ray emitter. If the group is the X-ray emitter, it has an $L_x = 6 \times 10^{42}$ ergs s^{-1} and $\log f_x/f_v = -0.8$; these values are typical for X-ray selected groups. The presence of several compact, perhaps tidally truncated, companions is also reminiscent of other X-ray selected groups like 1E 2316.2−4223 (Gioia *et al.* 1984). Only the detection of extended X-ray emission would indicate, beyond any doubt, that the group is indeed the optical counterpart of the X-ray source. The limited statistics of the detection, combined with virtually no information on the energy spectrum of the X-ray source, make the analysis of the X-ray surface brightness distribution inconclusive.

If the QSO is the source of the X-rays, its luminosity is $L_x = 4 \times 10^{45}$ ergs s^{-1} (0.3–3.5 keV; $q_0 = 0$), and $\log f_x/f_v = 0.53$ ($\alpha_{ox} = 1.26$; see Tananbaum *et al.* 1979 for the definition of α_{ox}). This value of α_{ox} may seem to indicate unusually strong X-ray emission when compared with the values found for other radio-quiet QSOs (e.g., Zamorani *et al.* 1981) or for other broad absorption-line QSOs (Bregman, Huggins, and Glassgold 1982). An α_{ox} value of 1.26 is not so extreme, however, when compared with the α_{ox} distribution of X-ray selected QSOs (Chanan, Margon, and Downes 1981; Stocke *et al.* 1983*b*; Gioia *et al.* 1984). About 25% of all X-ray selected QSOs are characterized by a value of α_{ox} equal to or smaller than 1.26.

Conclusive evidence that the QSO is the correct identification for 1E 0104.2+3153 would have come only from a high-resolution imager (HRI) detection of a pointlike source coincident with the optical image of the QSO. The detection of X-ray variability (regardless of whether the variability is intrinsic to the QSO or due to a transient gravitational lensing of the QSO continuum induced by halo stars in the elliptical galaxy; see § V for a detailed discussion of this point) would be substantial but not conclusive proof for the QSO identification because if the X-ray source were dominated by nuclear emission from galaxy A, it could also be variable.

An HRI image scheduled as a follow-up observation of 3C 31 and containing the region around 1E 0104.2+3153 was taken on 1981 February 15. However, no source is detected from the vicinity of 1E 0104.2+3153, and this exposure sets a 5 σ upper limit of 3.8×10^{-13} ergs cm^{-2} s^{-1} to the flux of a pointlike source at that position. Taken at face value, the HRI upper limit suggests variability in the X-ray flux of 1E 0104.2+3153. However, flux comparison between the HRI and IPC instruments should be done only with extreme caution, primarily because the different energy response of the two instruments makes the conversion between HRI and IPC count rates a strong function of the assumed incident spectrum and of the assumed interstellar and intrinsic absorption. The HRI flux upper limit was derived assuming the same power-law slope ($\alpha = -1.5$) and galactic absorption ($n_H = 3 \times 10^{20}$ cm^{-2}) as was assumed to obtain the IPC flux for this source. Also, this particular upper limit is derived from counts in a region close to the edge of the HRI detector, where corrections due to vignetting, broadening of the point-spread function, and coma amount to 50%–60%. Therefore, there is as yet no strong evidence for X-ray variability from 1E 0104.2+3153, so we will have to wait for future X-ray observations to resolve the ambiguity of the optical counterpart to this X-ray source. The forthcoming X-ray satellite *ROSAT* has the capability to do so.

There is one further, *a posteriori* argument worth noting. If the galaxy group is the X-ray emitter, then the presence of the QSO in the X-ray error circle is truly a chance coincidence. However, if the QSO is the X-ray emitter, its detection may have been favored by a transient gravitational lensing of the QSO continuum region by halo stars in the elliptical galaxy. In this case, the alignment of the QSO and the galaxy may have been necessary to produce the observed X-ray flux, and consequently, neither object is there by chance.

III. CCD PHOTOMETRY OF THE FIELD

Figure 1 is a 10 minute CCD frame of the 1E 0104.2+3153 field taken on 1982 February 21 with the MMT in 2″ seeing through an F filter ($\lambda_c = 6500$ Å; $\Delta\lambda = 1500$ Å; see Schild and Kent 1981 for photometry reduction technique and transformation to standard systems). A "de Vaucouleurs

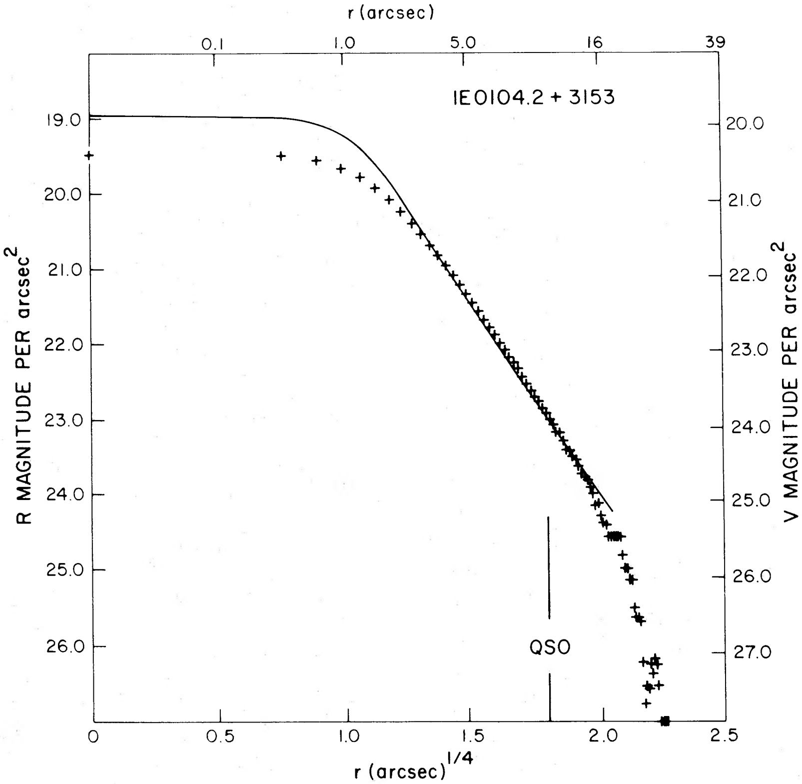

FIG. 2.—The brightness profile of galaxy A in the 1E 0104.2+3153 field obtained from Fig. 1. The + signs mark the actual values in either the R or V band (see Table 3); the solid curve is the best fit de Vaucouleur profile described in the text. The vertical line marks the exact position of the QSO relative to the galaxy center although its brightness has been removed from this plot to display the galaxy brightness distribution only.

profile" has been fitted to the radial brightness of galaxy A using a least-squares fitting program written by S. Kent (see Fig. 2). Although well fitted by the de Vaucouleurs law for the bulk of its radius, this galaxy has a 0.5 mag deficiency inside 3" and a slight deficiency for $r > 15''$ as well. Lowering the sky value by 1% would give a much improved fit, but such a low sky value is not permitted by our direct determination from star-free areas on the CCD frame. In any case, there is no indication of a break in the brightness profile to a flatter slope as is seen outside the nuclear regions of S0s and spiral galaxies (Holmberg 1975). In addition, there is no indication of any clumpiness in the brightness distribution of galaxy A on a B-filter CCD frame kindly taken for us by Drs. H. Arp and J. Sulentic on the Kitt Peak National Observatory (KPNO) 4 m, thus increasing our confidence that this is indeed an elliptical galaxy.

Because of the aforementioned departures from a de Vaucouleurs law, it is very difficult to choose an appropriate best fitting brightness profile. Our least-squares fitting procedure always determines a best fit by an iterative procedure, but the fit depends somewhat upon the choice of endpoints. We have fixed the seeing FWHM at 2".1 (seven pixels) and have not fitted the inner 2".5 diameter portion of the profile. We also did not fit the profile beyond 17" radius to force the main body of the galaxy to dominate the fit. Our final fitting parameters are summarized in Table 2. Because the galaxy is poorly fitted by the standard de Vaucouleurs law, we also list in Table 3 the detailed brightness profile as measured from the CCD frame.

To compare the total luminosity of galaxy A with other galaxies, we compute directly the visual absolute magnitude to the 26th magnitude isophote. From the calibration of the photometry and from our measured profile, we find that the $V = 26$ mag isophote occurs at a radius of 19".4, and the visual magnitude within this isophote is $V = 16.02$. In these calculations we adopt from Schild and Oke (1971) the standard redshifted elliptical galaxy colors $(V-R) = 0.89$ and $(B-R) = 2.20$ for $z = 0.11$. Also, for this redshift we adopt from Schild and Oke (1971) a K-correction of $\Delta V = 0.16$, and from Burstein and Heiles (1982) we adopt the absorption correction $E(B-V) = 0.05$. These data combine to yield a corrected absolute visual magnitude $M_v(26) = -22.0$. Since Figure 2 shows that the surface brightness of galaxy A is falling very steeply at the 26th magnitude isophote, this

TABLE 2

1E 0104.2+3153 ELLIPTICAL GALAXY PROPERTIES

Diameter of 26th V magnitude isophote	$D(26) = 39''$ (64 kpc)
Magnitude to 26th V magnitude isophote	$R(26) = 15.13$ ($M_R = -21.9$)
Effective radius	r(eff) = 8".5 (13.8 kpc)
Central surface brightness	$B_0(V) = 21.6$
QSO impact parameter	$b = 10''.0$ (16.3 kpc) $= 1.18r$(eff)

TABLE 3

1E 0104.2+3153 ELLIPTICAL GALAXY PROFILE

r(arcsec)	σ(R)	r(arcsec)	σ(R)
0	19.5	12.09	23.4
0.93	19.7	13.02	23.6
1.86	20.1	13.95	23.8
2.79	20.5	14.88	24.1
3.72	20.9	15.81	24.4
4.65	21.3	16.74	24.6
5.58	21.7	17.67	24.6
6.51	22.0	18.60	25.0
7.44	22.3	19.53	25.2
8.37	22.5	20.46	25.8
9.30	22.8	21.39	27.0
10.23	23.0	22.32	27.0
11.16	23.2	23.25	27.0
		24.18	...

isophotal magnitude must be almost equal to the total magnitude. Thus this galaxy is intermediate in brightness between the average Sandage (1973) brightest rich-cluster elliptical galaxies ($M_v = -21.8$) and the poor-cluster cD galaxies ($M_v = -22.2$; Thuan and Romanishin 1981), but it is not as bright as rich-cluster cD galaxies like NGC 6166 ($M_v = -24.9$; Oemler 1976). Because galaxy A does not have an extended halo, it can in any case not be considered a cD galaxy. But it is certainly a giant elliptical, albeit with a somewhat truncated outer profile.

The distance of the QSO from the center of the elliptical galaxy has been determined to sub-arcsecond precision by determining the photometric center of each object individually. First and second moments of each brightness distribution within 3″ diameter apertures were synthesized and solved for the image center and eccentricity. The small synthetic aperture was chosen to ensure that the brightness gradient of the galaxy halo did not affect the position determined for the QSO image. Our result is that the QSO-galaxy separation is 10″.0 ± 0″.1, which is 1.2 times the de Vaucouleurs effective radius of the elliptical galaxy. At this distance from the center, the elliptical galaxy has a surface brightness of $V = 23.9$ mag arcsec^{-2}.

IV. THE BROAD ABSORPTION-LINE (BAL) QUASAR

a) *The Broad Absorption Lines*

The spectrum of object B in Figure 1 is shown in Figure 3, a composite of five separate spectra taken with the Steward 2.3 m spectrograph with blue-sensitive, intensified Reticon detector and the MMT spectrograph with intensified Reticon detector (Latham 1982) during the 1982 and 1983 observing seasons. The partially overlapping spectral coverage causes the signal-to-noise ratio to vary considerably across Figure 3, with the highest signal-to-noise ratio occurring in the crucial 4150–4750 Å region. Throughout the entire range the resolution has been degraded to a uniform 10 Å FWHM, corresponding to the resolution of the single lowest resolution scan.

Based upon the emission lines of C III], C IV, Si IV, and N V, the QSO redshift is $z_{em} = 2.027 \pm 0.001$. That Lyman-α is not seen in emission is presumably due to the deep "P Cygni" absorptions of N V λ1240, a characteristic nearly unique to the BAL QSOs. Object B does, in fact, meet all of the criteria to be classified as a BAL QSO (Weymann, Carswell, and Smith,

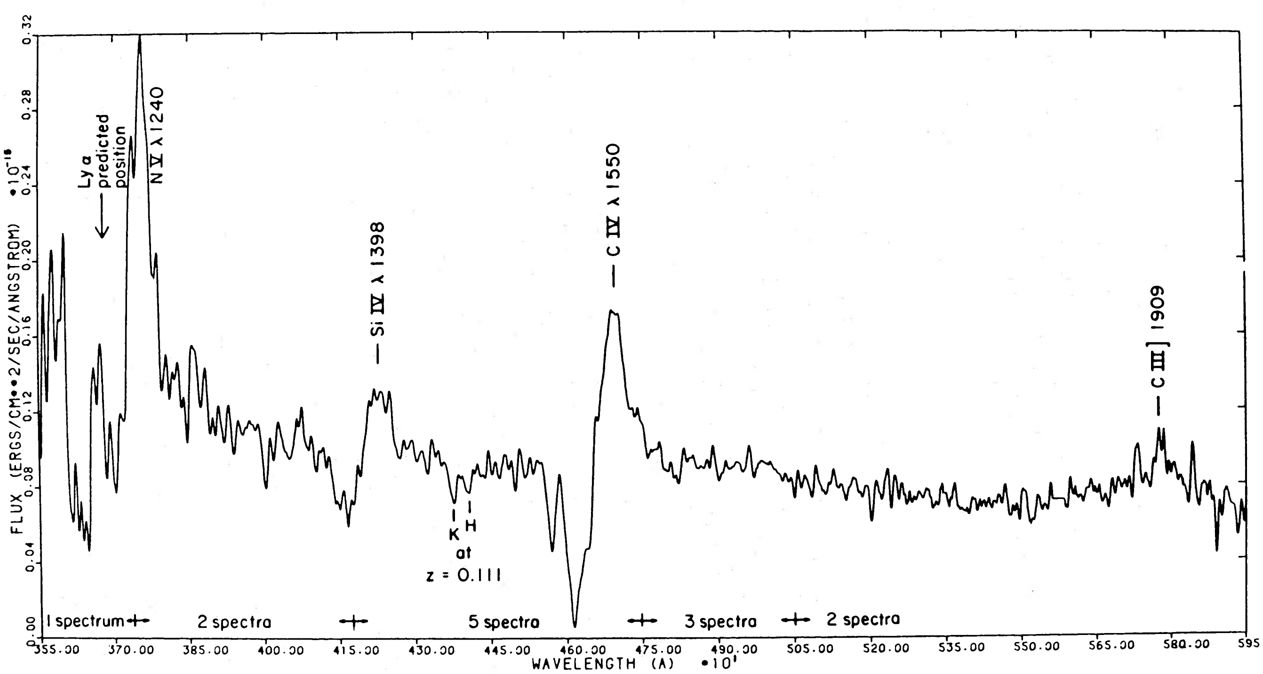

FIG. 3.—The optical spectrum of object B in Fig. 1, the broad absorption-line QSO. This spectrum (Δλ = 10 Å) is a composite of five individual spectra taken with the Steward 2.3 m and MMT during the 1982 and 1983 observing seasons. Because of the composite nature of this spectrum, the signal-to-noise ratio varies considerably across the wavelength coverage and is highest in the 4150–4750 Å region, which contains the probable Ca II H and K absorptions at the redshift of galaxy A.

TABLE 4

POSITIONS OF EMISSION AND ABSORPTION FEATURES IN FIGURE 3

Wavelength (Å)	Spectral Feature	z	Velocity Relative to z_{em} (km s^{-1})
3603.2	N V blue abs. edge	1.906	−12,000
3630.1	N V abs. #2	1.928	−9800
3690.0	N V abs. #1	1.976	−5050
3755.0	N V emission	2.028	0
4080.6:	Si IV blue abs. edge	1.921:	−10,500:
4103.5:	Si IV abs. #2	1.937:	−8900:
4155.0	Si IV abs. #1	1.974	−5250
4230.3	Si IV emission	2.028	0
4376.7 (4375.5)[a]	Ca II K	0.1126 (0.1123)[a]	…
4406.4 (4408.8)[a]	Ca II H	0.1103 (0.1110)[a]	…
4550.2	C IV blue abs. edge	1.933	−9300
4569.1	C IV abs. #2	1.946	−8000
4612.8	C IV abs. #1	1.974	−5250
4693.5	C IV emission	2.026	0
5779.0	C III] emission	2.027	0

[a] Values for central 2″.5 of galaxy A shown in parentheses; $\langle z \rangle = 0.1115 \pm 0.0005$ for galaxy A determined from Ca II H and K, G band, Mg *b* λ5176, and Na D.

1981, hereafter WCS) including the requirements for "contiguous" absorption that is greater than 2000 km s^{-1} in breadth and whose blue edge is displaced at least 5000 km s^{-1} blueward from the emission-line center (see Table 4). This QSO shows a dominant BAL trough (absorption system #1 in Table 4) with consistent trough velocities amongst the three species. However, the C IV, Si IV, and N V velocities are not in good agreement for a weaker, second trough (system #2) nor for the extreme blue absorption edge. We do not consider these differences significant for Si IV because of the relatively poor signal-to-noise ratio in that spectral region compared with the weakness of the features. For N V the presence of possible Lyα absorption and a rapidly changing continuum level blueward of the Lyα emission position may be responsible for the poor agreement with C IV. Thus, this BAL QSO is not particularly extreme or unique (see Turnshek 1981 and WCS).

b) *The Absorptions Due to the Foreground Galaxy*

The most unusual feature of this already somewhat unusual QSO spectrum is the pair of absorption lines near 4400 Å. These lines have the correct wavelengths, approximate spacing (±9 Å), and relative strengths to be Ca II H and K absorption lines from the interstellar medium of the foreground *elliptical* galaxy, object A. Indeed, as the insert to Figure 1 and Figure 2 indicate, the QSO is well within the envelope of galaxy A. Within rather large errors the recession velocity of the H and K lines in the QSO spectrum (33,450 ± 450 km s^{-1}) is identical to the nuclear velocity of galaxy A (33,450 ± 150 km s^{-1}, from a spectrum obtained at the MMT). Note particularly that the reality of these two features must be judged relative to the signal-to-noise ratio in the 4150–4750 Å region only; the continuum blueward of that region is much noisier because only two spectra taken with the Steward 2.3 m contribute. We further note that the proposed H and K absorptions appear on each of the four highest signal-to-noise spectra, and that a statistical treatment of these four spectra yields 3.8 σ and 3.2 σ levels of significance for the K and H lines, respectively. We, therefore, consider that these absorption lines are almost certainly real but require confirmation and further study at higher signal-to-noise ratio and resolution.

There are four independent arguments that these absorption lines cannot be due to a starlight contribution from the galaxy itself:

1. The relative strengths of these two absorption features are those expected for unsaturated lines at low density. In stars, these lines have approximately equal strengths, the high-density limit; in galaxies, because of the blending of Ca II H and Hε, the H line is often stronger. This is, in fact, the case in the nuclear spectrum of galaxy A.

2. Figure 2 shows that at the QSO position the galaxy is ~24th magnitude arcsec^{-2} in *V* band. Correcting this value to *B* band using the observed galaxy spectrum and conservatively assuming that all the QSO spectral data was obtained through 2″.5 circular apertures (the largest used to produce Fig. 3), the galaxy contributes less than 3% of the quasar continuum at 4400 Å.

3. The galaxy spectrum contains a continuum break just redward of H and K which the QSO spectrum does not have. The amount of the galaxy continuum break and the observed noise level of the QSO spectrum permits less than 6% of the QSO continuum to be due to the galaxy. There is also no indication of galaxy continuum farther to the red and no indication of G band or Mg *b* absorption lines either.

4. Assuming only that the deepest BAL of C IV (system #1) is not produced by absorbing material between us and galaxy A, the contribution of the continuum of galaxy A to the QSO spectrum is limited to less than the flux at the blackest point in that line (<5%). In fact, in the two 4 Å resolution spectra which contribute to Figure 3, the C IV BAL at λ4613 reaches zero intensity, further restricting the starlight contribution.

One may argue that these lines are a third and fourth BAL system of C IV intrinsic to the quasar because some BAL QSOs have absorption extending to −30,000 km s^{-1} with respect to the emission lines. However, we consider this unlikely because:

1. The position and spacing would match Ca II H and K in galaxy A purely by chance.

2. The associated Si IV absorptions at λλ3933, 3958, and 3985 are not present; we note, however, that the signal-to-noise ratio is poorer in that region of Figure 3, and thus their presence is not absolutely excluded by present data.

We have presented these detailed arguments to clearly eliminate other possible identifications for the absorption lines near λ4400 because if indeed they are interstellar lines arising in galaxy A, they are enormously strong: EW = 2.1 and 1.2 Å for K and H, respectively! These EWs are a factor of 2 larger than the largest yet seen in other QSO-galaxy alignments. The previous record was held by a probable S0 galaxy (Blades, Hunstead, and Murdock 1981; EW = 1 and 0.4 Å), which led to a column density of $N(\mathrm{Ca}^+) = 11(+5, -3) \times 10^{12}$ cm^{-2} and a Doppler width of $b = 90 \pm 20$ km s^{-1}. In comparison, the LMC line of sight to 30 Doradus has

$N(\mathrm{Ca}^+) = 6\text{–}8 \times 10^{12}$ cm^{-2} (Blades 1980). For galaxy A we obtain $N(\mathrm{Ca}^+) \gtrsim 3 \times 10^{13}$ cm^{-2} and $b \approx 150$ km s^{-1} (Strömgren 1948). The estimated uncertainties in each of the EWs of the Ca$^+$ lines in Figure 3 are 25%. So the range of possible EW ratios is so large that it includes the low-density limit, which yields the column density quoted above and an uncertainty in b that is as large as the quoted value for b. Although these two lines appear marginally resolved in Figure 3, we conservatively estimate FWHM < 8 Å, implying $b < 500$ km s^{-1}. Clearly these widths—both measured and derived—cannot be thermal, and so we must be viewing this particular QSO through several clouds in galaxy A.

Since the heavy-metal abundance in halo gas is very poorly understood (York 1982), we assume a Ca abundance one-tenth solar (i.e., Population II abundance with no grain depletion of Ca). We further assume that there is no nearby source of energetic photons, so that all the Ca is once ionized to obtain a $n(\mathrm{H}) > 1.7 \times 10^{20}$ cm^{-2} for the quasar line of sight through galaxy A. The nature of the above assumptions requires that this $n(\mathrm{H})$ value is a firm lower limit; again strongly suggesting that there are several interstellar clouds in the continuum beam of this QSO.

If these H and K absorptions can be confirmed at higher signal-to-noise ratio and resolution so that individual components can be resolved, we will be faced with the surprising result that the highest column densities of interstellar gas between us and individual QSOs have been found in early-type galaxies. Why is this gas not forming stars? Also, if many clouds do contribute to these lines, their velocity dispersion will lead to a very accurate measurement of the M/L ratio in this giant elliptical galaxy (Faber and Gallagher 1979). Clearly, higher dispersion observations of this QSO are desirable.

If this order-of-magnitude column density were spread uniformly throughout galaxy A, it would contain more than $10^9\ M_\odot$ of neutral hydrogen. Although a uniform distribution of H I is unlikely, a 21 cm search for H I emission from galaxy A is nevertheless in order. Since neither the elliptical galaxy nor the QSO is an appreciable radio source (<0.5 mJy; Gioia *et al.* 1983; Stocke *et al.* 1983*a*), a search for H I absorption against a continuum source (as has been so successful both for galaxies and for quasars; Dressel, Bania, and Davis 1983 and references therein) is not possible in this case.

V. GRAVITATIONAL LENSING OF THE BAL QSO BY FOREGROUND HALO STARS

The gravitational field of the giant elliptical galaxy (object A) and its associated group brightens the QSO image by only a few tenths of a magnitude, much less than occurs if the lensing galaxy is approximately halfway to the QSO (e.g., Young *et al.* 1980). Also, because of the relative distance of this QSO-galaxy pair, the deflections due to the galaxy group are much too weak to produce multiple images. In the context of the discussion below, the light amplification due to the galaxy and cluster is weak and constant and does not significantly alter the geometry for the transient effects due to stars we now discuss.

Although gravitational focusing of distant objects by individual stars has been discussed for many years (Einstein 1936), these ideas have been recently rediscussed for stars in galaxies intermediate between us and QSOs. In particular, Chang and Refsdal (1979), Gott (1981), and Young (1981) have discussed light variations in the "Twin Quasars" (Weymann *et al.* 1979) due to the passage of individual stars in the lensing galaxy (Young *et al.* 1980) near the quasar continuum beams. If a star passes within a distance r_0 of the line of sight, the so-called Einstein ring radius, it can cause a brightness enhancement ($\Delta m \gtrsim 0.1$ mag) of the image over a time scale of (here we use the notation of Young 1981)

$$\Delta t = \frac{r_0}{v_t}\left(\frac{D_s}{D_{ds}}\right) = \frac{1}{v_t}\left(\frac{4GM_*}{c^2}\frac{D_d D_{ds}}{D_s}\right)^{1/2}\left(\frac{D_s}{D_{ds}}\right), \tag{1}$$

and dramatic transient "flares" ($\Delta m \gtrsim 1$ mag) can occur if the star passes directly through the beam, r_b, with a time scale of

$$\delta t = \frac{r_b}{v_t}\left(\frac{D_s}{D_{ds}}\right) = \frac{r_q}{v_t}\left(\frac{D_d}{D_s}\right)\left(\frac{D_s}{D_{ds}}\right), \tag{2}$$

where r_0 is the radius of the luminous ring, which occurs only if the passing star intercepts the line of sight; r_b is the size of the beam as it passes the deflecting star; r_q is the physical size of the emitting region (0.01 pc assumed here for illustration); v_t is the transverse velocity of source, deflector, and observer (we use $v_t = 600$ km s^{-1} here for illustration; see Gott 1981 and Young 1981 for detailed discussions of this point); M_* is the stellar mass; D_s, D_d, and D_{ds} are the source, deflector, and source-to-deflector distances, respectively. The factor of (D_s/D_{ds}) corrects the time scale from the deflector to the observer plane (Chang and Refsdal 1979).

Table 5 lists values for the parameters in equations (1) and (2) for the Twin Quasars, the QSO discussed herein, and a typical distant QSO ($z \approx 1$) found projected close to a nearby galaxy (e.g., Arp 1981). Also listed is an estimate of the mean distance on the sky between stars near the QSO line of sight using the prescription in Young (1981):

$$r_c = \left(\frac{M_*}{\pi\Sigma}\right)^{1/2}, \quad \text{where} \quad \Sigma = \frac{\sigma_v^2}{2Gr}; \tag{3}$$

where Σ is the surface density of stars in the line of sight; σ_v is the central velocity dispersion of the galaxy in question; r is the galactocentric radius of the QSO line of sight. Equation (3) assumes that all the galactic matter is in stars, and that the mass distribution is that of an isothermal sphere. Therefore, particularly at large galactocentric distance, the actual r_c could be considerably less than the values obtained from equation (3). In the case of 1E 0104.2+3153 we confirm the value of r_c obtained using equation (3) and listed in Table 5 using the photometry in Figure 1 and conservatively assuming $M/L = 1\ M_\odot/L_\odot$ (all the *visible* mass is in stars). If the dynamical mass found in galaxies (typically $M/L > 10$) is in the form of low-mass stars, then r_c will be smaller than as quoted here. Also note the dependence of r_0, r_c, and (r_b/r_c) on M_* and H_0.

The ratios $(r_0/r_c)^2$ and $(r_b/r_c)^2$ are measures of the probability that a single star is within r_0 and r_b, respectively, and thus the probability that the quasar image is enhanced or dramatically enhanced at the present time. As Young (1981) has previously noted, the lensing effects of individual stars badly overlap for the Twin Quasar images, and the problem of brightness enhancements is no longer as simple as the single-

TABLE 5

HALO STAR LENSING OF DISTANT QUASARS

Parameter	Q0957+561 (Image B)/(Image A)	1E 0104.2+3153	Typical "Arp" Quasar	Notes
D_s (Mpc)	1242	1336	1000	
D_d (Mpc)	725	283	10	
D_{ds} (Mpc)	720	1169	1000	
r_0 (pc)	9×10^{-3}	7×10^{-3}	1.4×10^{-3}	1
Δt (yr)	28	11	2.2	1, 2
r_b (pc)	1×10^{-2}	2×10^{-3}	1×10^{-4}	3
δt (yr)	30	3	1/6	2
r_c (pc)	$1 \times 10^{-2}/2.5 \times 10^{-2}$	2×10^{-2}	$1.7\text{–}5.6 \times 10^{-2}$	1
at a galactocentric distance of (kpc)	@3.5/@19	@16	@10–100	
$(r_0/r_c)^2$	0.8/0.16	0.12	$0.007\text{–}7 \times 10^{-4}$	
$(r_b/r_c)^2$ for $M_* = M_\odot$	1/0.2	0.01	3×10^{-5} to 3×10^{-6}	4
$(r_b/r_c)^2$ for $M_* = 0.1\,M_\odot$	10/2	0.10	3×10^{-4} to 3×10^{-5}	4

NOTES.—(1) Scales as $(M_*/M_\odot)^{1/2}(H_0/100)^{-1/2}$. (2) For $V_t \approx 600$ km s^{-1}. (3) For $r_q \approx 0.01$ pc. (4) Scales as $(M_*/M_\odot)^{-1}(H_0/100)$.

star case discussed by Chang and Refsdal (1979) and Gott (1981). Also note that only in the Twin Quasar case is $r_b \approx r_0$; because only in this case do the galaxy and cluster amplify the images significantly (estimated factors of 6 and 4 for the A and B1 images, respectively; Young *et al.* 1980) providing a larger beam in the observer's plane. These long time scales for large brightness variations are borne out by Young's Monte Carlo simulations. On the other hand, nearby bright galaxies have extremely small values of r_0/r_c and r_b/r_c and thus extremely small probabilities that enhancement is currently taking place. Canizares (1981) and Keel (1982) have suggested that these small probabilities of enhancement coupled to the steep $N(m_v)$ relation for QSOs account for the excess numbers of QSOs reported near bright galaxies (e.g., Burbidge *et al.* 1971; Arp 1981).[3]

The QSO-galaxy pair 1E 0104.2+3153 is intermediate between these two extreme cases and presents us with our best opportunity to directly observe changes in the brightness of a QSO image as stars move in or out of the beam in the manner predicted by Einstein (1936). The ~3 yr time scale and 1%–10% probability that a flare is in progress are obtained assuming a QSO continuum emission region (r_q) of 0.01 pc (10 lt-day). A smaller emission region lowers δt but also lowers the probability of a flare.

The amplitude of the brightness enhancement (A) also scales with the size of the emitting region ($A \propto r_q^{1/2}$; Chang and Refsdal 1979), but flares much more than doubling the light output are still expected even for $r_q \approx 0.1$ pc. However, given the larger canonical size of the broad emission-line region (~1 pc), the emission lines will vary only a few percent during a flare (although the broad absorptions will follow continuum variations). In this manner extrinsic variations due to lensing mimic the expectation for intrinsic variations (Gott 1981).

The amplitude of any dramatic continuum flare also depends on the *mass* of the deflecting star (Einstein 1936) as $A \propto (M_*/D_d)^{1/2}$. So although there is a greater probability for a low-mass star to be in the beam, its corresponding effect on the brightness of the image is somewhat less. However, since $A \propto (M_*/D_d)^{1/2}$, the effect of a 1 $M_\odot$ star on image A or B in 0957+561 is the same as the effect an 0.4 $M_\odot$ star has on 1E 0104.2+3153. To gain an impression of the magnitude of any brightness enhancements we refer the reader to trial #1 in Young (1981), for which no magnification or shearing is contributed by the overall galaxy or cluster gravitational potentials. For 1E 0104.2+3153 the ratio r_b/r_0 is always small for any reasonable choice of r_q (the values in Table 5 correspond to $\sigma = 0.3$ in Young's parameterization). For such a situation, the mean amplification is a factor of 4 with approximately a 30% chance of $A > 6$. Since Young's computer simulations were for a star of $M_* = 1\ M_\odot$ in the geometry of the Twin Quasars, they closely correspond to the expectations for a 0.4 $M_\odot$ star in the case analyzed here. Thus again this particular QSO-galaxy pair seems better suited to observing brightness fluctuations due to low-mass stars than any other known alignment.

We further remark that although there is no second image to help separate intrinsic from extrinsic variations in this case, the expected brightness fluctuations are larger than any intrinsic QSO variability except those occasionally seen in the few optically violent variable (OVV) quasars. Up to now the OVVs have been exclusively strong radio sources, while this BAL QSO is undetected at centimeter wavelengths (<0.5 mJy; Stocke *et al.* 1983*a*). For this reason we expect that any large flares detected must be viewed as extrinsic in nature.

However, no dramatic variations in brightness have yet been detected in this QSO. Using the POSS, two plates obtained on the Palomar 5 m on 1964 October 9/10 and 1968 September 30/October 1 by H. Arp, an image-tube plate

[3] However, Keel points out that the absence of any long-term brightness fluctuations in the "Arp QSOs" requires that the deflecting objects have $M_* > 10\ M_\odot$ to raise the Δt shown in the fourth column of Table 5 to values consistent with the historical absence of variability in these QSOs.

obtained on the Steward 2.3 m on 1981 November 1/2, the CCD frame shown in Figure 1, and one CCD frame obtained by H. Arp on the KPNO 4 m on 1983 February 9/10 revealed no brightness fluctuations greater than 0.5 mag in the quasar image. Since we lack images of this field obtained within 1 yr of the *Einstein* IPC observation of 3C 31, we reiterate the *possibility* that the X-ray satellite caught the quasar in an extrinsic flaring state due to the passage through the line of sight of a foreground halo star in galaxy A. Further optical monitoring of this field is now in progress.

We wish to thank Drs. H. Arp and J. Sulentic for the loan of plate material for our inspection. Drs. C. Foltz and B. Wilkes are thanked for assistance with their exquisite spectral reduction software. We also thank Dr. John Geary, who has developed and maintained CCD cameras for direct imaging at the F. L. Whipple Observatory. J. T. S. and J. W. L. acknowledge the continuing support of NASA grant NAG-8442. This work has received partial financial support from NASA contract NAS8-30751 and from the Italian PSN (Piano Spaziale Nazionale). Drs. Richard E. White and Fred Chaffee are thanked for several helpful discussions.

REFERENCES

Arp, H. 1981, *Ap. J.*, **250**, 31.
Blades, J. 1980, *M.N.R.A.S.*, **190**, 33.
Blades, J., Hunstead, R., and Murdock, H. 1981, *M.N.R.A.S.*, **194**, 669.
Boksenberg, A., Danziger, I. J., Fosbury, R., and Goss, W. 1980, *Ap. J. (Letters)*, **242**, L145.
Boksenberg, A., and Sargent, W. L. W. 1978, *Ap. J.*, **220**, 42.
Bregman, J., Huggins, P., and Glassgold, A. 1982, *Bull. AAS*, **14**, 648.
Burbidge, E. M., Burbidge, G., Solomon, P., and Strittmatter, P. 1971, *Ap. J.*, **170**, 233.
Burstein, D., and Heiles, C. 1982, *A.J.*, **87**, 1165.
Canizares, C. 1981, *Nature*, **291**, 620.
Chanan, G. A., Margon, B., and Downes, R. A. 1981, *Ap. J. (Letters)*, **234**, L5.
Chang, K., and Refsdal, S. 1979, *Nature*, **282**, 561.
Dressel, L., Bania, T., and Davis, M. 1983, *Ap. J. (Letters)*, **266**, L97.
Einstein, A. 1936, *Science*, **84**, 506.
Faber, S., and Gallagher, J. 1979, *Ann. Rev. Astr. Ap.*, **17**, 135.
Gioia, I., Feigelson, E. D., Maccacaro, T., Schild, R., and Zamorani, G. 1983, *Ap. J.*, **271**, 524.
Gioia, I., Maccacaro, T., Schild, R., Stocke, J., Liebert, J., Danziger, J., Kunth, D., and Lub, J. 1984, *Ap. J.*, submitted.
Gott, R. 1981, *Ap. J.*, **243**, 140.
Haschick, A., and Burke, B. 1975, *Ap. J. (Letters)*, **200**, L137.
Holmberg, E. 1975, in *Stars and Stellar Systems*, Vol. **9**, *Galaxies and the Universe*, ed. A. Sandage, M. Sandage, and J. Kristian (Chicago: University of Chicago Press), p. 123.
Jarvis, J., and Tyson, J. 1981, *A.J.*, **86**, 476.
Keel, W. 1982, *Ap. J. (Letters)*, **259**, L1.
Latham, D. 1982, in *IAU Colloquium 67*, *Instrumentation for Astronomy with Large Optical Telescopes*, ed. C. M. Humphries (Dordrecht: Reidel), p. 259.
Maccacaro, T., *et al.* 1982, *Ap. J.*, **253**, 504.
Oemler, A. 1976, *Ap. J.*, **209**, 693.
Sandage, A. 1973, *Ap. J.*, **183**, 743.
Schild, R., and Kent, S. 1981, in *SPIE Symposium 290*, *Solid State Imagers for Astronomy*, ed. J. Geary and D. Latham (Bellingham, Wash.), p. 186.
Schild, R., and Oke, J. 1971, *Ap. J.*, **169**, 209.
Stocke, J., Foltz, C., Weymann, R., and Christiansen, W. 1983*a*, *Ap. J.*, submitted.
Stocke, J. T., Liebert, J., Gioia, I. M., Griffiths, R. E., Maccacaro, T., Danziger, I. J., Kunth, D., and Lub, J. 1983*b*, *Ap. J.*, **273**, 458.
Strömgren, B. 1948, *Ap. J.*, **108**, 242.
Tananbaum, H., *et al.* 1979, *Ap. J. (Letters)*, **234**, L9.
Thuan, T., and Romanishin, W. 1981, *Ap. J.*, **248**, 439.
Turnshek, D. 1981, Ph.D. thesis, University of Arizona.
Weymann, R. J., Carswell, R., and Smith, M. 1981, *Ann. Rev. Astr. Ap.*, **19**, 41 (WCS).
Weymann, R. J., Chaffee, F. H., Jr., Davis, M., Carleton, N. P., Walsh, D., and Carswell, R. F. 1979, *Ap. J. (Letters)*, **233**, L43.
York, D. 1982, *Ann. Rev. Astr. Ap.*, **20**, 221.
Young, P. J. 1981, *Ap. J.*, **244**, 756.
Young, P. J., Gunn, J. E., Kristian, J., Oke, J. B., and Westphal, J. A. 1980, *Ap. J.*, **241**, 507.
Zamorani, G., *et al.* 1981, *Ap. J.*, **245**, 357.

I. M. GIOIA, T. MACCACARO, and R. SCHILD: Center for Astrophysics, 60 Garden Street, Cambridge, MA 02138

JAMES LIEBERT and J. T. STOCKE: Steward Observatory, University of Arizona, Tucson, AZ 85721